

Contents lists available at ScienceDirect

# Transportation Research Part C

journal homepage: www.elsevier.com/locate/trc





# Empirical study on car-following characteristics of commercial automated vehicles with different headway settings<sup>★</sup>

Xiaowei Shi, Xiaopeng Li\*

Department of Civil and Environmental Engineering, University of South Florida, Tampa, FL 33620, USA

#### ARTICLE INFO

Keywords:
Automated Vehicles
Adaptive Cruise Control
Car Following
Safety
Mobility
Stability
Empirical Method

#### ABSTRACT

A recent study (Li, 2020) analytically predicted tradeoffs between automated vehicle (AV) following characteristics on safety, mobility, and stability using a parsimonious linear carfollowing model. This work aimed to verify the key theoretical findings in the above study with empirical experiments using commercial AVs, e.g., vehicles with adaptive cruise control (ACC) functions. We collect high-resolution trajectory data of multiple commercial AVs following one another in a platoon with different headway settings. Parsimonious linear AV-following models that capture the first-order parameters on safety, mobility, and stability aspects are estimated with the data. The estimation results of the key parameters validate several theoretical predictions predicted by Li (2020). Specifically, it was found that as the time lag setting increases, the corresponding safety buffer decreases, indicating that AV safety could be improved with less pursuit of AV mobility or, conversely, AV mobility improvement may come at a cost of more stringent safety requirements. Also, as the time lag setting increases, AV string stability increases, indicating that stop-and-go traffic potentially could be dampened by compromising AV mobility. With this, one possible explanation to the observed string instability of commercial AV following control (i.e., ACC function) is that automakers may prefer to ensure a relatively short headway (and thus better user experience on vehicle mobility) at a cost of compromising string stability. It was also found that as the time lag increases, the cycle period of traffic oscillations gets longer, and the oscillation amplification gets smaller, which supports the tradeoff between mobility and stability. On the other hand, field experiments revealed issues beyond the predictivity of a simple linear model. That is, vehicle control sensitivity factors vary across different speed and headway settings, and the model estimation results for key parameters are not consistent over different speed ranges. This opens future research needs for investigating nonlinearity and stochasticity in the AV following modeling.

## 1. Introduction

Automated vehicle (AV) technology holds great potential to improve traffic safety, comfort, and energy optimization (Li and Li, 2019; Naranjo et al., 2008; Qu et al., 2020; Shi and Li, 2019; Wang et al., 2019) and thus is considered one of the most promising transportation technologies in the near future. AV following control, as a fundamental function of AV at all automation levels (SAE,

E-mail addresses: xiaoweishi@usf.edu (X. Shi), xiaopengli@usf.edu (X. Li).

<sup>&</sup>lt;sup>★</sup> This article belongs to the Virtual Special Issue on IG005581: VSI:MFTS.

<sup>\*</sup> Corresponding author.

2020), has significant impacts on road traffic performance, including both stationary (e.g., vehicle-following headway) and dynamics (e.g., traffic oscillation) characteristics. Clear understandings of the impacts of AVs on road traffic provide informative insights into academia and industry, such as traffic simulation, product development, and road traffic management, etc.

In general, a vehicle-following spacing, i.e., the distance between the front bumpers of the two consecutive vehicles, can be decomposed into three components – the preceding vehicle length, a time-lag gap, and a safety buffer, as illustrated in Fig. 1 (Li, 2020). The time lag is reserved for response delay and driving comfort, and the safety buffer is reserved to absorb the overshoot caused by the following vehicle due to the uncertainty of the preceding vehicle's movements. Due to the mechanical nature of the AV- following control, the relatively long time-lag gap caused by human drivers was expected to be largely reduced by the control of AV (Karaaslan et al., 1990), and thus the corresponding mobility performance such as road capacity would be significantly improved as well. However, based on state-of-the-art studies in the literature, the road capacity of AV traffic was found comparable or even worse than that of human-driven vehicle traffic under specific headway settings of AV (Shi and Li, 2020; Shladover et al., 2012). These findings challenged the expected lucrative benefits of AV technology predicted in research (Kesting et al., 2008; Makridis et al., 2020a).

One possible reason for the discrepancy between theoretical predictions and industry practice is that the existing AV-following control design is string unstable. Vehicle string (or asymptotic) stability investigates whether the perturbations of a lead vehicle of a vehicle string get amplified while propagating across multiple following vehicles in the vehicle string. The string instability will cause traffic oscillation and a consequential road capacity drop due to the increased space between vehicles (Chen et al., 2014); e.g., a small speed perturbation of a preceding vehicle will be amplified while propagating across multiple following vehicles and may even lead to stop-and-go traffic. The other potential reason is safety concerns. Due to the uncertainty of the preceding vehicle's movements, to guarantee a sufficient safety buffer for absorbing the worst-case following AV overshoot considering all possible movements of the preceding vehicle, vehicle makers might set a safety buffer to a relatively conservative value at a cost of compromising AV mobility and decreasing road capacity (Li, 2020; Milanes et al., 2014).

Studies investigating the impacts of AV-following control designs on road traffic performance (i.e., safety, mobility, stability) are abundant (Ghiasi et al., 2017; Jerath and Brennan, 2012; Kesting et al., 2010; Ngoduy, 2013; Seiler et al., 2004; Talebpour and Mahmassani, 2016). For example, Ghiasi et al. (2017) proposed a Markov chain-based traffic capacity model to study the impacts of AVs with different penetration rates on mixed traffic. Kesting et al. (2008) presented an adaptive cruise control strategy in which the driving style can be automatically adjusted according to traffic scenarios, and the potential impacts of the strategy on traffic were analyzed. However, most of these studies validated their findings by using simulation-based approaches (Lenard, 1970; Treiber and Kesting, 2013), and only a few conducted corresponding field experiments. Due to the lack of empirical validations, some findings obtained with simulation approaches, e.g., AVs can significantly improve traffic stability and road capacity, were inconsistent with those from field experiments (Gunter et al., 2020; Milanés and Shladover, 2014; Shi and Li, 2020), which highlighted the needs for using field experiments to scrutinize theoretical findings. In the literature, only a few studies (e.g., Ciuffo et al., 2020; Gunter et al., 2019; Knoop et al., 2019; Makridis et al., 2020b; Milanés and Shladover, 2014; Shi and Li, 2020; James et al., 2019) investigated following control designs of commercial AVs (or production vehicles that have automated control features such as adaptive cruise control) with field experiments. These studies showed that existing commercial AVs were string unstable. Despite these successes, none of them investigated the design considerations of the string-unstable design of commercial AV control, e.g., possibly as a compromise with factors such as safety and driving comfort (Eskandarian, 2003; Xiao and Gao, 2010).

Further, note that commercial AVs often offer users to customize the AV-following headway among different levels. Although the impacts of different headway settings on traffic mobility and stability could be significant, this issue was rarely investigated in the literature. To the best of the authors' knowledge, only Gunter et al. (2019) and Shi and Li (2020) are related to this topic. Gunter et al. (2019) calibrated an optimal velocity relative velocity car-following model with field experiment data and investigated the string stability of the calibrated model with two different headway settings. They found that even the AV-following design is string unstable, and commercial AV platoons of moderate size can dampen disturbances. However, only the results from two headway settings cannot provide a clear vision to the variation trend of the string stability. Compared with Gunter et al. (2019), Shi and Li (2020) studied the impacts of different headway settings on traffic from a macroscopic aspect and constructed a fundamental diagram for AV traffic with four different headway settings based on field experiment data. The results indicated that AV headway settings can affect traffic flow

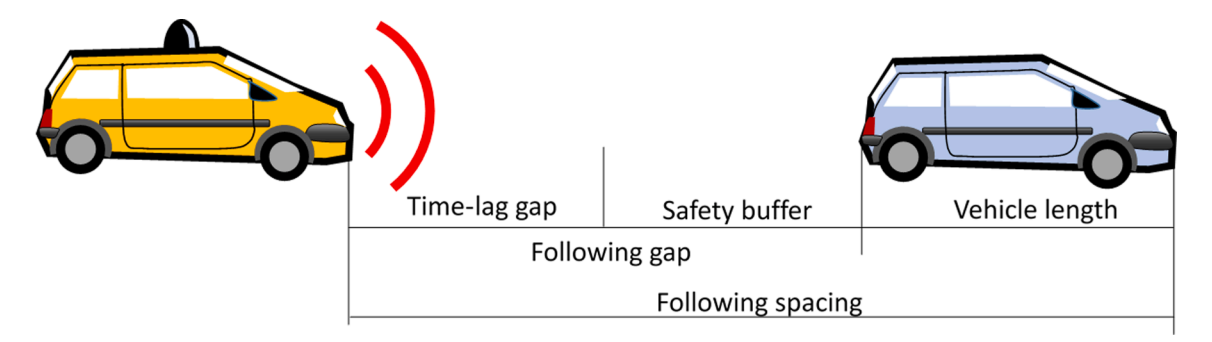


Fig. 1. Illustration of following spacing components.

Source: Li, 2020

stability. Although Shi and Li (2020) presented a successful study and revealed insights into the relationship between string stability and AV headway settings, they did not qualitatively analyze the relationship. Moreover, none of them incorporated traffic mobility into their research, which is quite relevant to traffic stability.

A recent study (Li, 2020) analytically explained the tradeoffs among safety, mobility, and stability of the underlying AV control mechanism by proposing a parsimonious linear AV-following model based on the above following spacing decompositions (i.e., preceding vehicle length, time-lag gap, and safety buffer). This study aimed to provide empirical support to the Li (2020) findings with field experiment data. Field experiments with commercial AVs with longitudinal automation were conducted to collect high-resolution AV-following trajectory data. Parameters of the parsimonious linear AV following model were estimated with linear regression using the collected trajectory data. Interestingly, the estimated parameters for the existing commercial AV-following design verify the following theoretical findings in Li (2020):

- 1) There exists a tradeoff between the time lag gap and the safety buffer that together constitute the AV- following gap and thus determine road capacity. As the time lag gap increases, the corresponding safety buffer decreases, indicating that AV safety could be improved with less pursuit of AV mobility or, conversely, AV mobility improvement may come at a cost of more stringent safety requirements.
- 2) There exists a relation between the time lag gap and AV string stability. As the time lag gap increases, AV string stability increases, i. e., with a smaller amplification ratio and a longer oscillation period. This indicates that the stop-and-go traffic potentially could be dampened by compromising AV mobility.
- 3) By theoretically solving the string stable headway setting for the studied AV following design, a possible explanation to the observed string instability of the design (i.e., adaptive cruise control [ACC] function) is that the string-stable headway would be too long to result in superior driving experience (e.g., cut-in lane changes may be induced by long headway). Thus, automakers may opt to design a relatively short headway for the best user experience (which may be directly correlated with users' vehicle purchase decisions) at a cost of compromising string stability (which could be perceived only when traffic oscillation is amplified across a platoon of vehicles).

Additionally, the estimated parameters reveal the following findings that were beyond what was reported in Li (2020):

- 1) It was found that the range of the lead vehicle's acceleration variation that the investigated linear AV control accommodates is rather narrow. When the lead vehicle's speed variation gets beyond this range, it is likely that the nonlinear control mechanism will be activated, which could largely reduce the needed safety buffer length and thus the linear model prediction becomes too conservative (Li and Ouyang, 2011). This seems also related to the above-speculated automakers' desire to reduce the needed safety following headway. Nonetheless, this finding indicates that the current commercial AV-following design entrusts much of the safety warranty to nonlinear control mechanisms (e.g., drastic emergency stops) while the linear control dominates only in a relatively narrow acceleration range. The revelation of this design mindset can help researchers understand the AV design components in which AV safety risks likely reside. Further, it may raise a need to introduce nonlinear AV control models in AV traffic analysis to better reflect AV safety performance; most existing AV traffic simulation studies rely on simplified linear models alone.
- 2) The estimated vehicle control sensitivity factors vary across different speed and headway settings, again alluding to nonlinear control mechanisms. This indicates that automakers opt to adjust the vehicle control sensitivity to fit different driving environments, possibly for better driving experience and vehicle performance.

Overall, this study validated the theoretical findings in Li (2020) with field experiment data. Also, additional managerial insights into the nonlinearity of existing commercial AV control design were drawn. It will be helpful for transportation stakeholders to better understand how emerging AV technology will impact traffic operations and for automakers to consider further improvements on the existing design.

The rest of this paper is organized as follows. Section 2 presents the designs of the field experiments for collecting the AV trajectory data. Section 3 introduces the linear AV-following model proposed in Li (2020) to be estimated with the collected data. Section 4 examines the relationships among the estimated parameters of the AV-following model to verify the tradeoffs between safety, mobility and stability and draw additional managerial insights. Section 5 concludes the paper and points out the directions for future research.

#### 2. Experiment designs and data collections

This section describes the detailed experiment designs for collecting the car-following trajectory data of state-of-the-art commercial AVs. The collected car-following trajectory data were used to estimate the models of the AV-following control design. All field tests were conducted on a segment of SR-56 in Florida with four lanes between Bruce B Downs Blvd and Gall Blvd during time periods when traffic was light.

#### 2.1. Vehicle fleet

The vehicles employed in the field experiments included two AVs equipped with commercially-implemented ACC systems and one regular vehicle equipped with a cruise control system. The AV models were Lincoln MKZs 2016 and 2017 with the same vehicle length (i.e., 4.92 m); the regular vehicle model was an Audi Q7. The equipped ACC systems of these two AVs were the same – four different

following headway settings, indexed from 1 through 4 as the headway increases. Note that the ACC systems in the AVs can also perform speed cruise control such that specified speed profiles can be executed by inputting the desired speed to the ACC systems. Therefore, these two ACC vehicles were used to collect the two-vehicle car-following data – one served as the preceding vehicle executing a specified speed profile and the other as the following vehicle. To collect three-vehicle platoon trajectory data, the Audi Q7 served as the leading vehicle and the Lincoln MKZ 2016 and 2017 were the second and third vehicles in the platoon following the leading vehicle in the ACC mode in a single lane. Trajectory data of vehicles during the experiments were recorded for further analysis.

#### 2.2. Data collection

Real-time GPS positions and speeds of the experiment vehicles were collected at a sampling rate of 1 Hz by high-accuracy u-blox C066-F9P GPS receivers with the antenna affixed to the rear bumper on each vehicle. Preliminary testing indicated that the GPS receivers had a position accuracy of 0.26 m and a speed accuracy of 0.089 m/s. Thus, the real-time vehicle-following spacing between the two vehicles could be obtained by the distance between the GPS positions of the two vehicles due to the identical lengths of the two vehicles.

#### 2.3. Two-Vehicle car following experiment designs

The goal of the two-vehicle car-following experiment was to study the AV-following characteristics for speed changes in the lead vehicle under different speed ranges and headway settings. Thus, in the experiment, the preceding AV executed 10 speed profiles for each headway setting (i.e., headway settings 1 through 4), and the following AV followed the preceding vehicle in a single lane. Of the 10 speed profiles, the first 5 were named as the high-speed range tests (45–55 mph) that have relatively higher vehicle speed, and the rest were named as the low-speed range tests (25–35 mph). Each speed profile was conducted twice for cross validation before proceeding to the next speed profile; thus, there were 20 tests for each headway setting. To help readers understand the test settings, the detailed test plan for headway setting 1 (i.e., Tests 1–20) is shown in Table 1.

Each test included 3 phases with identical durations (30 s). Each test started after both vehicles reached a given initial cruise speed (e.g., 55 mph for the first 10 tests in Table 1). In the first phase (i.e., first 30 s), the preceding vehicle cruised at the initial speed. In the second phase (30–60 s), the preceding vehicle changed its speed to a desired lower speed and then cruised at the desired speed for the rest of the time in this phase. In the third phase (60–90 s), the preceding vehicle changed its speed back to the initial speed and then cruised at the initial speed until the end of this phase. Note that two consecutive tests may share the phase, i.e., the third phase of the previous test being the first phase of the following test when these two phases are at the same desired speed. The ACC target speed of the preceding vehicle was manually set to the desired speed at the beginning of each phase. The following vehicle followed the preceding vehicle in the ACC mode with a sufficiently high target speed (e.g., 80 mph) that did not constrain the vehicle's acceleration or speed. With this, a total of 80 tests (20 for each headway setting) were conducted, and the recorded trajectory length was about 200 miles in total.

For illustration purposes, the raw speed data for the high-speed tests with different headway settings are shown in Fig. 2. Note that due to occasional disruptions (e.g., red light signals, end of test segment, downstream slow vehicles, etc.) from the public road where the tests were conducted, the collected data were not continuous at all times. Once an interruption occurred, the ongoing tests would be repeated to guarantee completion of the data collection. It is notable to mention that the publicly available datasets that include different headway settings were extremely limited. To the best of the authors' knowledge, only Gunter et al. (2019) generously shared their dataset that includes two headway settings, which may not be sufficient to study the relationship among AV-following characteristics and headway settings. Our dataset bridges this gap by including four levels of headway settings.

#### 2.4. Three-Vehicle platoon experiment designs

To supplement the above data in particular to test oscillation periodicity, a series of three-vehicle platoon tests were conducted, in which the speed of the lead vehicle was changed periodically to match the dominating oscillation periods derived for the estimated AV control models (see Table 4 for estimated period values).

Table 1
Test Plan for Each Headway Setting.

Test number	Initial speed (mph)	Target speed (mph)	Test number	Initial speed (mph)	Target speed (mph)
1	55	53	11	35	33
2	55	53	12	35	33
3	55	51	13	35	31
4	55	51	14	35	31
5	55	49	15	35	29
6	55	49	16	35	29
7	55	47	17	35	27
8	55	47	18	35	27
9	55	45	19	35	25
10	55	45	20	35	25

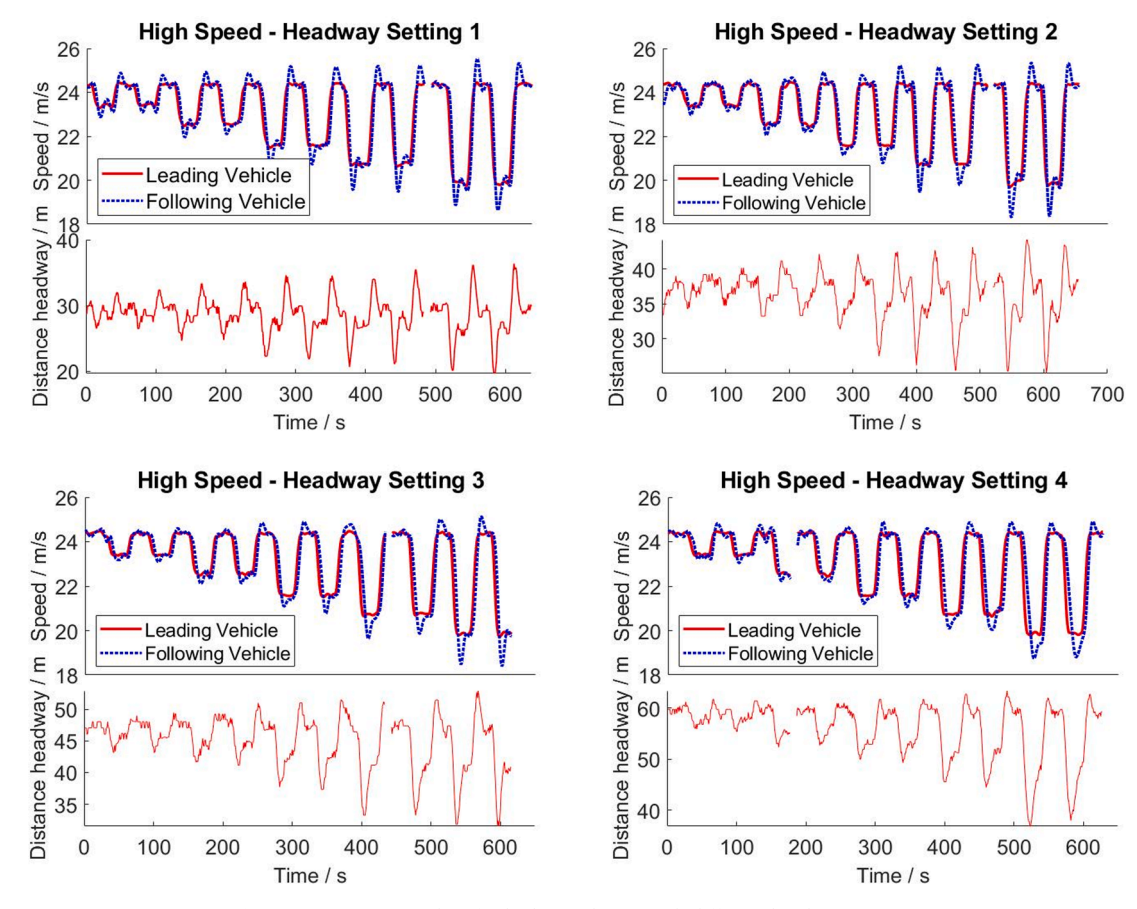


Fig. 2. Raw trajectory data for high-speed tests with different headway settings.

As noted, the Audi Q7 was the lead vehicle, and the Lincoln MKZs 2016 and 2017 were the second and third vehicles in the platoon following the lead vehicle in the ACC mode in the same lane. For each headway setting, five different cycle periods were tested -18, 20, 22, 24, and 26 s. Each period was repeated in four cycles to reveal the propagation pattern of the repeated cyclic speed profile while attenuating the impacts of the initial states. Therefore, the duration time for the tests with one headway setting was (18+20+22+24+26)\*4=440 seconds. The two target speeds of the lead vehicle were set to 55 mph and 50 mph. The lead vehicle's speed profile was generated by manually setting its cruise control target speed to the corresponding target speed at the beginning of each half cycle, i.e., 50 mph for the first half of a cycle and 55 mph for the second half of a cycle. As a result, the lead vehicle speed decreased from 55 mph to 50 mph in the first half of each cycle and increased from 50 mph to 55 mph in the second half of a cycle. To help readers understand the test settings, the detailed test plan for headway setting 1 with a cycle period equal to 18 s is shown in Table 2 as an example. Since the cycle period will be repeated four times, the duration time was 72 s for the example.

The obtained raw speed data with different headway settings are shown in Fig. 3. Analysis of the platoon data is elaborated on in the stability analysis section.

**Table 2**Test Plan for Headway Setting 1 with Cycle Period Equal to 18 Seconds.

Cycle number	Duration (seconds)	Initial speed (mph)	Target speed (mph)	
1	1–9	55	50	
1	10–18	50	55	
2	19–27	55	50	
2	28–36	50	55	
3	37–45	55	50	
3	46–54	50	55	
4	55–63	55	50	
4	64–72	50	55	

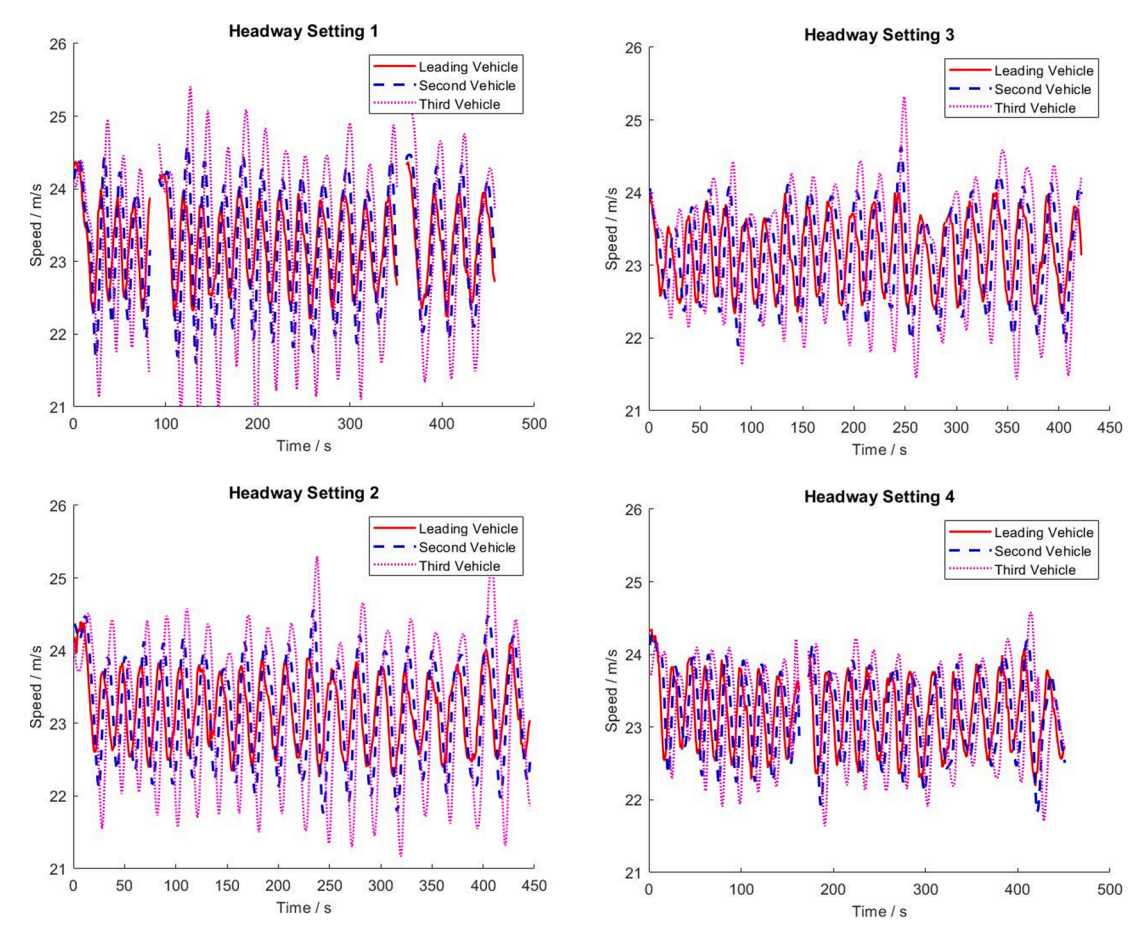


Fig. 3. Raw trajectory data for platoon tests with different headway settings.

#### 3. Car-following model

This study adopted the parsimonious linear AV following model proposed in Li (2020) for estimating associated AV control parameters in different settings. This model was formulated as shown in Equation (I)

$$\ddot{y}(t) = k[x(t) - l - \Delta - y(t) - \tau \dot{y}(t)], \tag{1}$$

where x(t) and y(t) are the locations (of the front bumpers) of the preceding and following vehicles at time t, k > 0 is the control sensitivity factors,  $\Delta \ge 0$  is the safety buffer,  $\tau \ge 0$  is the time lag, l > 0 is the fixed preceding vehicle's length, and the dot and double dot operators are the first- and second-order derivatives, respectively.

The above model is actually the linearized form of the optimal-velocity car-following model proposed to explain periodic traffic oscillation (Bando et al., 1995). As argued in Li et al. (2012), the above linear structure was adopted for the following reasons. First, a linear structure well describes vehicle-following behavior when vehicle speed oscillation is relatively small. Secondly, the performance of a linear AV control model was verified by several field experiments (Gunter et al., 2020; Milanés and Shladover, 2014). Further, the proposed linear structure is arguably the simplest form that captures all safety (with  $\Delta$ ), mobility (with the following spacing  $x(t) - l - \Delta - y(t) - \tau \dot{y}(t)$ ) and stability (e.g., as a second-order feed-back control with sensitivity factors k) aspects in a physically meaningful way (Li, 2020).

The above simple linear model has certain limitations. First, the linear model may not capture possible nonlinear effects in AV control. Further, the model does not contain the speed difference term compared with the general second-order linear model used in describing AV-following behavior. However, it may still be valuable to conduct an analysis with these limitations. Li and Ouyang (2010) showed that a linear model likely overestimates actual speed oscillation and, thus, the safety buffer obtained from a linear model tends to be on the conservative side and actually provides an upper bound of the actually needed safety buffer, which is acceptable for safety analysis. Further, the data fitness result in Section 4.1 suggests that the impacts on model predictability of dropping the speed difference term are minor in terms of the adjusted  $R^2$ . Separate numerical tests also showed that dropping this term does not much affect the control overshoot that determines the safety buffer value. Thus, dropping the speed difference term does not lose much generality for this study.

#### 4. Field data fitness results and analyses

This section estimates the parameter values of the AV control model (I) with the experiment data collected in Section 2. The relationships between the estimated parameters in different settings are discussed to test the theoretical findings in Li (2020) and draw additional insights. Section 4.1 presents the estimated parameters. Sections 4.2 and 4.3 analyze the mobility and string stability implications of the AV following design, respectively. Section 4.4 provides discussion beyond the theoretical predictions of Li (2020). Section 4.5 verifies the relations among the estimated parameters by experiment data collected by Gunter et al. (2019). To avoid term confusion, some terms are defined before the analyses. In this paper, "headway" refers to the time separation between two consecutive vehicles' front bumpers, "gap headway" refers to the time separation between the leading vehicle's rear bumper to the following vehicle's front bumpers, and "spacing gap" refers to the distance between the leading vehicle's front bumper.

#### 4.1. Data fitness results

The simple moving average method with a window of 5 s was used to denoise the collected data before parameter estimations. By fitting each set (for each headway setting at one speed range) of the two-vehicle car-following data, such as x(t), y(t),  $\dot{y}(t)$  and  $\ddot{y}(t)$ , to model (I) with linear regression that aims to maximize the adjusted  $R^2$  value, a total of eight sets of estimation results are obtained as shown in Table 3. To verify that the proposed parsimonious linear AV-following model can capture the vehicle following behavior without much loss of predictability, the adjusted  $R^2$  value of the general second-order linear AV control model with the speed difference term is also provided as a benchmark in Table 3 (BM.  $R_{adi}^2$ ). The benchmark model is formulated in Equation (II).

$$\ddot{y}(t) = k_1 [x(t) - l - \Delta - y(t) - \tau \dot{y}(t)] + k_2 [\dot{x}(t) - \dot{y}(t)], \tag{2}$$

where  $k_1, k_2 > 0$  are the control sensitivity factors, and the definitions of the other parameters are the same as those in parsimonious model (I).

Comparing the adjusted  $R^2$  of the two models shows that the impacts on the model predictability of dropping the speed difference term from the benchmark model are minor. We see that the adjusted  $R^2$  values for parsimonious model (I) across all the settings are above 0.82, which indicates a fairly good predictability of this model. Further, the improvements of the adjusted  $R^2$  from parsimonious model (I) to benchmark model (II) are not significant. Thus, it does not lose much of the generality to use parsimonious control model (I) in the analysis instead of the general second-order control model (II).

With the estimated parameter values (i.e.,  $\tau$ , k, and  $\Delta$ ), the acceleration ranges (denoted by  $[-\overline{a}, \overline{a}]$ ) for the studied AV following design were calculated by plugging the estimated parameter and the speed variation ranges (denoted by  $[\nu_-, V]$ ,  $\nu_-=8.94$  m/s for the studied AV following design, and V=24.59 m/s or 15.65 m/s that is dependent on the experiment settings) into the equation proposed in Li (2020) (i.e., Equation [16] in Li (2020)), and the results are summarized in Table 3.

It can be observed in Table 3 that the calculated acceleration ranges are very narrow. The average acceleration range over the eight estimations is [-0.495, 0.495] m/s2. This means that for the studied AV-following design, the proposed linear model can well interpret the AV following behavior only when the acceleration is within [-0.495, 0.495] m/s2. This result indicates that the current commercial AV following design entrusts much of safety warranty to nonlinear control mechanisms (e.g., drastic emergency stops) while the linear control only dominates in a relatively narrow acceleration range. This finding raises cautions of using linear models to describe ACC behavior in simulation, which is pretty much most traffic simulation does.

#### 4.2. Mobility and safety analysis

This section interprets the parameter estimation results obtained in Table 3 from the mobility and safety perspectives and verifies the corresponding theoretical predictions in Li (2020). HS refers to short of the high-speed results and LS refers to short of the low-speed results in the following figures. Fig. 4 (a) plots the estimated  $\tau$  values over the headway settings. By fitting the scatters to a simple linear regression model, it is clear that the headway settings are highly correlated with the estimated time lags in a linear relationship. The  $R^2$  of the fitted straight lines for both the high-speed and low-speed settings are over 0.985, indicating very good fitness. The results are consistent with the expectation that the corresponding time lag gap of the commercial ACC system increases

**Table 3**Data Fitness Results for Proposed Parsimonious Model and Benchmark Model.

	τ(s)	k	$\Delta(m)$	$R_{adj}^2$	$BM.R_{adj}^2$	$[\nu,V]$ (m/s)	$[-\overline{a},\overline{a}](m/s^2)$
High Speed-Headway Setting 1	0.83	0.10	4.83	0.87	0.90	[8.94, 24.59]	[-0.46, 0.46]
High Speed-Headway Setting 2	1.21	0.10	4.40	0.95	0.96		
High Speed-Headway Setting 3	1.61	0.09	3.31	0.92	0.93		
High Speed-Headway Setting 4	2.17	0.07	0.66	0.84	0.86		
Low Speed-Headway Setting 1	0.79	0.12	7.28	0.92	0.93	[8.94, 15.65]	[-0.53, 0.53]
Low Speed-Headway Setting 2	1.14	0.09	6.36	0.90	0.92		
Low Speed-Headway Setting 3	1.52	0.08	5.92	0.83	0.86		
Low Speed-Headway Setting 4	2.09	0.08	4.97	0.82	0.82		

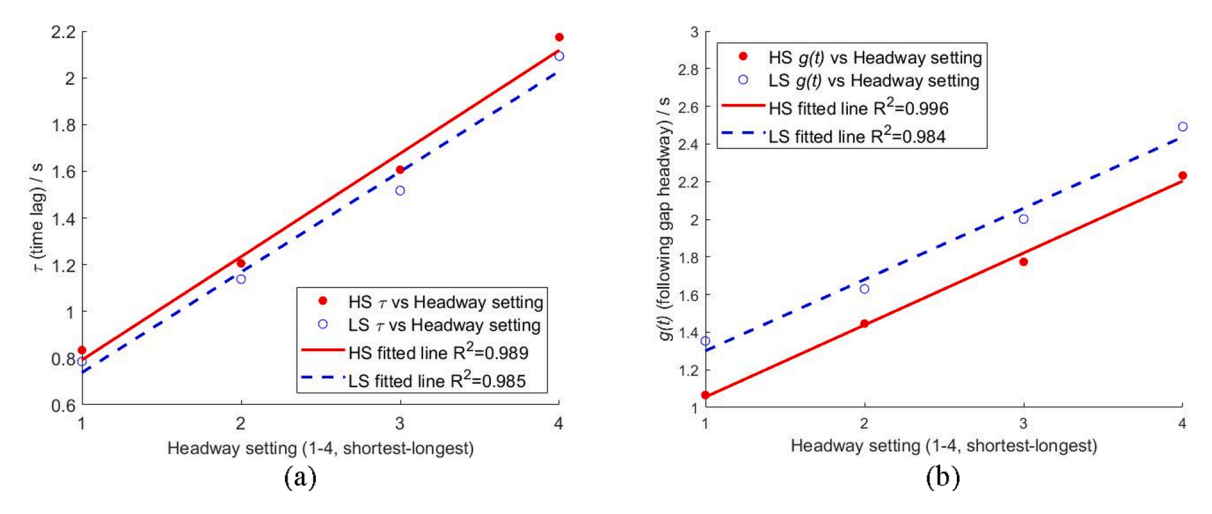
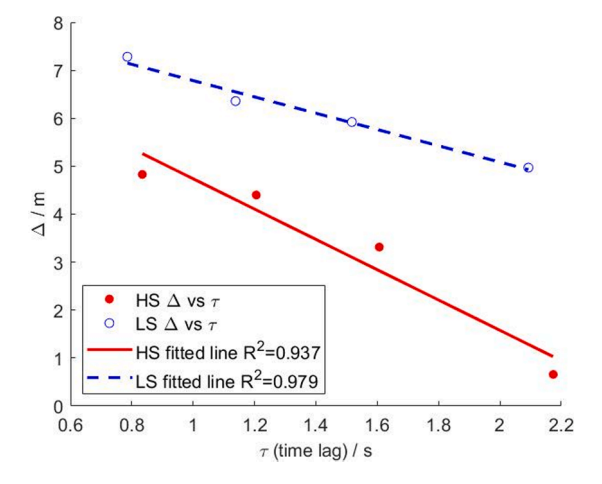


Fig. 4. (a) Scatter plot of  $\tau$  vs headway setting, 4 (b) scatter plot of following gap headway (g(t)) vs headway setting.

linearly with the headway settings. However, of note is that although it was found that there is a linear relationship between the time lag gap and headway settings for the studied ACC system (Lincoln brand), the time lag gap may not necessarily be a linear scaling from the headway settings 1-4. Different vehicle vendors can have different design strategies for the headway settings while the linear relationship perhaps is the simplest strategy. Further, the results between the high-speed and low-speed settings are consistent, indicating that the time lag is relatively fixed at the same headway setting across all speed ranges. Based on the following gap decompositions as shown in Fig. 1,  $g(t) = \tau + \Delta/\dot{y}(t)$ , where g(t) and  $\dot{y}(t)$  are the following gap headway (inter-gap headway) and following vehicle speed at time t, respectively. Fig. 4 (b) shows the values of the average following gap headway (calculated by averaging the measured following gap headway across all time intervals in an experiment setting, i.e.,  $\sum_{t=1}^{T} g(t)/T$ , where T is the number of time intervals) over the headway settings. It can be found that there is also a linear relationship between the values of average following gap headway and the headway settings. Moreover, the fitted line for low-speed settings is slightly higher than the fitted line for high-speed settings as shown in Fig. 4 (b). Since the values of the time lag (i.e.,  $\tau$ ) are relatively fixed, it indicates that the safety buffer headway ( $\Delta/\dot{y}(t)$ ) for the low-speed settings are greater than that of the high-speed settings, which is consistent with the estimated results in Table 3.

Fig. 5 shows how  $\Delta$  (i.e., safety buffer) varies with  $\tau$ . It can be observed in Fig. 5 that as  $\tau$  increases,  $\Delta$  always decreases for both high-speed and low-speed settings. This suggests that a shorter time-lag gap (i.e.,  $\tau$ ) demands a longer safety spacing buffer (i.e.,  $\Delta$ ) to absorb a higher overshoot from the target trajectory in the vehicle following control. This verifies the theoretical finding proposed in Li (2020) that there exists a tradeoff between the time lag gap and the safety buffer. In addition, it was found that the slope of the fitted lines of the high-speed settings is steeper than that of the low-speed settings, which indicates that for the studied ACC design, the variations of  $\Delta$  regarding  $\tau$  at high-speed conditions are more sensitive than that at the low-speed conditions. An interesting finding regarding Fig. 5 is that the average  $\Delta$  for the low-speed settings is greater than that for the high-speed settings. It means that the overshoot of the vehicle following at high-speed conditions is less than that at low-speed conditions, indicating certain nonlinearity of the AV following control.



**Fig. 5.** Scatter plot of  $\Delta$  vs  $\tau$ .

Moreover, the tradeoff between safety buffer  $\Delta$  and time lag  $\tau$  shown in Fig. 5 also has an implication on road capacity. Consider a one-lane road with pure AVs following the vehicle control model specified by model (I); it is easy to see that the minimum headway or equivalently the maximum traffic throughput occurs when the traffic is at the following optimal equilibrium state, i.e., all vehicles driving at the speed limit, V, with a minimum following spacing gap of  $\tau V + \Delta$ . The value of V is set to the maximum speed for each experiment setting. Let  $\tau^*$ ,  $\Delta^*$ , and  $g^*$  denote the optimal time lag, safety buffer, and following gap headway to the minimum headway or the maximum traffic, where  $g^* := \tau^* + \Delta^* / V$ . Then,  $\tau^*$ ,  $\Delta^*$ , and  $g^*$  can be theoretically solved by the equation and a bisecting search method proposed in Li (2020) (Equation (16) in Li (2020)). Table 4 shows the key parameters of the minimum headway settings and those of the studied AV following design. A smaller headway setting reduces the time lag (i.e.,  $\tau^*$ ) but increases the safety buffer (i.e.,  $\Delta^*$ ) to achieve shorter following gap headways (i.e.,  $g^*$ ) as well as higher traffic capacity compared with the studied AV following design.

#### 4.3. Stability analysis

Unstable AV-following design may easily cause traffic oscillation and, consequentially, road capacity may drop, which reduces the service level of the road. To determine whether the estimated models for the studied AV following design are stable or not, this section investigates the stability of the estimated AV following models based on the formulation (i.e., model (I)).

Note that this study particularly focused on the empirical analyses, and the following theoretical analyses are a brief revisitation of Section 6 of Li (2020). By applying the Laplace transform to model (I), we obtain

$$\frac{Y(s)}{X(s)} = \frac{k}{s^2 + k\tau s + k}, \forall s \in \mathbb{C},$$

where  $X(s) := \int_0^\infty x(t)e^{-st}dt$ ,  $Y(s) := \int_0^\infty y(t)e^{-st}dt$ , and  $\mathbb C$  is the set of complex numbers. The roots of the above equation are  $(-k\tau \pm \sqrt{k^2\tau^2 - 4k})/2$ . With this, if  $k\tau^2 < 4$ , model (I) is a local stable AV following model. Based on the data fitness results as shown in Table 3, we conclude that all estimated model results are locally stable and thus the studied AV following design is locally stable. By applying the Fourier transform to model (I), we obtain

$$TF(w) := \frac{Y(jw)}{X(jw)} = \frac{k}{-w^2 + k + ik\tau w}, \forall w \in \mathbb{R}^+,$$

where  $j := \sqrt{-1}$ . Then we obtain

$$TF^* := \max_{w \in \mathbb{R}^+} |TF(w)| = \begin{cases} \sqrt{\frac{4}{4k\tau^2 - k^2\tau^4}} > 1, ifk\tau^2 < 2; \\ 1, ifk\tau^2 \ge 2, \end{cases}$$

with the maximizer angular frequency

$$w^* := \begin{cases} \sqrt{4k - 2k^2\tau^2} / 2, ifk\tau^2 < 2; \\ 0, ifk\tau^2 \ge 2. \end{cases}$$

Based on the analysis in Li (2020), if the value of  $k\tau^2 < 2$ , the perturbations of a preceding vehicle get amplified while propagating across multiple following vehicles; Otherwise, the perturbations of the preceding vehicle will be dampened across upstream and thus the AV following model is string stable. Note that if the model is string-unstable, small speed perturbations at the preceding vehicle will be amplified to cyclic speed oscillations with angular frequency  $w^* := \sqrt{4k - 2k^2\tau^2}/2$  (or cycle period  $T^* := 2\pi/w^*$ ) at the downstream following vehicles. With this, the parameters related to the stability of the fitted models are calculated as shown in Table 5.

It was found that the values of  $k\tau^2$  of all estimated results were less than 2, which indicates that the estimated AV following models are string unstable. This result is consistent with the previous studies' findings (Gunter et al., 2020; Milanés and Shladover, 2014). However, it was found that as the headway settings (i.e.,  $\tau$ ) increase, the values of  $k\tau^2$  increase as well and thus lead the increases of

Key Parameter Comparisons Among Studied AV Following Design, Minimum Headway Settings, and String Stable Headway Settings.

	Studied A	Studied AV following design			Minimum headway setting			String stable headway setting		
V(m/s)	$\Delta(m)$	τ(s)	g(s)	$\Delta^*(m)$	$\tau^*(s)$	g*(s)	Δ_(m)	τ_(s)	g_(s)	
24.45	4.83	0.83	1.02	5.43	0.24	0.46	0.59	4.47	4.50	
24.47	4.40	1.21	1.38	5.43	0.24	0.46	1.10	4.47	4.52	
24.48	3.31	1.61	1.74	5.87	0.26	0.50	1.69	4.71	4.78	
24.54	0.66	2.17	2.20	7.42	0.30	0.60	2.38	5.35	5.44	
15.49	7.28	0.79	1.24	3.81	0.26	0.51	0.72	4.08	4.13	
15.38	6.36	1.14	1.54	4.76	0.32	0.63	1.06	4.71	4.78	
15.43	5.92	1.52	1.89	5.35	0.34	0.69	1.54	5.00	5.10	
15.43	4.97	2.09	2.40	5.20	0.34	0.68	1.72	5.00	5.11	

**Table 5**Model Stability Related Parameters.

	$k\tau^2$	w*	<i>T</i> *(s)	Stability
High Speed-Headway Setting 1	0.07	0.31	19.99	Unstable
High Speed-Headway Setting 2	0.15	0.31	20.58	Unstable
High Speed-Headway Setting 3	0.24	0.29	22.04	Unstable
High Speed-Headway Setting 4	0.35	0.25	25.39	Unstable
Low Speed-Headway Setting 1	0.07	0.34	18.62	Unstable
Low Speed-Headway Setting 2	0.11	0.29	21.78	Unstable
Low Speed-Headway Setting 3	0.19	0.28	22.77	Unstable
Low Speed-Headway Setting 4	0.37	0.26	23.90	Unstable

cycle periods, which implicate that a higher  $\tau$  value, even if still resulting in string-unstable control, will increase the oscillation cycle period.

To support this implication, we designed an experiment as introduced in Section 2 to obtain the oscillation cycle period and amplification of the studied AV following design. Since each following vehicle will amplify its immediately preceding vehicle's frequency components in the neighborhood of  $w^*$  (or cycle period  $T^*$ ), the most-amplified preceding trajectory will have a sinusoidal speed profile with an angular frequency of  $w^*$ . Thus, the oscillation cycle periods of the studied AV following design can be obtained by T that has the largest oscillation amplification. As introduced, a series of three-vehicle platoon trajectory data are collected as shown in Fig. 3. For each headway setting of the AV, based on the calculated  $T^*$  shown in Table 5, five cycle periods were tested, such as T=18, 20, 22, 24, and 26 s.

The speed standard deviation ratio with different headway settings and cycle periods (i.e., *T*) that reflects the oscillation amplification for the third vehicle is shown in Table 6. The speed standard deviation ratio was calculated by the speed standard deviation of the third vehicle in the platoon dividing the speed standard deviation of the leading vehicle. Detailed theoretical analysis about this term can be found in the stability analysis section of Li (2020).

As shown in Table 6 that for headways 1–4, the largest speed standard deviation ratios of the third vehicle appear at  $T=20 \, \text{s}$ , 20 s, 22 s, and 26 s, respectively, which indicate that the  $T^*$  (i.e., speed oscillation cycle period) for each highway setting under high-speed condition is in the neighborhood of the obtained T. Also shown in Table 5, the high speed  $T^*$  for headways 1–4 respectively are 19.99 s, 20.58 s, 22.04 s, 25.39 s. This consistency between the practice results obtained from three-vehicle platoon data and the theoretical results obtained from two-vehicle car-following data support the above implication that as  $\tau$  increases, the oscillation cycle period  $T^*$  increases. Also, as observed in Table 6, the average speed standard deviation ratios decrease as the headway settings increase. This means that as  $\tau$  increases, the oscillation amplifications decrease, which also can be observed in Fig. 3. Therefore, we can further extend our finding that although the AV following design in the existing commercial vehicle is string-unstable, as  $\tau$  (i.e., headway setting) increases, the AV string stability increases in terms of the oscillation amplification and cycle periods.

As proposed in Li (2020), when  $\tau^2 k < 4$ , the riskiest cycle period  $\overline{T}$  of stop-and-go traffic that causes minimum gaps between two continuous vehicles is close to  $2\pi/\phi$ , where  $\phi$  is the angular frequency for the riskiest traffic, and  $\phi = \sqrt{4k - k^2\tau^2}/2$ . The platoon data is also used to check this finding. By plugging k and  $\tau$  in Table 3 into the equation of  $\phi$ , the riskiest cycle period for headway settings 1 to 4 under high-speed conditions are 0.31, 0.31, 0.29, and 0.25, which are the same with  $w^*$  because the values of  $k^2\tau^2$  are too small to cause differences between  $\overline{T}$  and  $T^*$ , and thus  $\overline{T} = T^*$ . Table 7 shows the 95% percentile shortest gaps between leading and second vehicles, and second and third vehicles with different headway settings and cycle periods. Note that the shortest gap for the gaps over five cycle periods (i.e., T=18, 20, 22, 24, 26 s) is marked with "\*".

As shown in Table 7, most of the shortest gaps for headway settings occur when T is in the neighborhood of  $\overline{T}$ . This result supports the finding that if the cycle period of stop-and-go traffic is close to  $2\pi/\phi$ , the gap between the AV and preceding vehicle can reach the shortest gaps and thus the AV control is subject to relatively high safety risks.

Additionally, Li (2020) proposed the equation to analytically solve the parameter settings of a string stable headway (i.e., time lag  $\tau$ -, safety buffer  $\Delta$ -, and following gap headway g-) based on the estimated parameters of the AV following design (i.e., k). Table 4 compares the key parameters of the string stable headway settings and those of the studied AV following design. It can be seen in Table 4 that the following gap headways of string stable headway settings (i.e., g-) are much greater than those of the studied AV following design (i.e., g). Together with the results of the minimum headway settings (i.e.,  $\tau^*$ ,  $\Delta^*$ , and  $g^*$ ), we see that there is a significant difference between the minimum headway settings and string stable headway settings that require much longer following gap headway and time lag but less safety buffer. This result indicates that string stability achieves at a cost of longer minimum

**Table 6**Speed Standard Deviation Ratio for the Third Vehicle.

	T = 18 s	T = 20 s	T = 22 s	T = 24 s	T = 26 s
Headway 1	1.304	1.553	1.505	1.515	1.478
Headway 2	1.378	1.460	1.403	1.446	1.424
Headway 3	1.270	1.215	1.440	1.253	1.352
Headway 4	1.142	1.199	1.201	1.148	1.208

Table 7
95% Percentile Shortest Gaps Between Leading and Second Vehicles and Second and Third Vehicles with Different Headway Settings and Cycle Periods.

	Leading and second vehicles					Second and third vehicles				
	T=18  s	T = 20 s	T = 22 s	T = 24 s	T = 26 s	T=18  s	T = 20 s	T = 22 s	T = 24 s	T = 26 s
Headway 1	24.48	20.50*	21.54	23.52	20.56	16.85	15.99*	17.57	18.71	16.48
Headway 2	30.25	30.57	27.89*	28.55	29.32	26.18	26.46	23.77*	26.46	24.68
Headway 3 Headway 4	39.19 48.33	38.23 49.52	38.21* 49.54	38.25 49.97	38.39 47.83*	36.24 46.87	34.72 46.48	35.51 46.69	33.12* 47.56	35.19 40.91*

headway. This explains why the existing commercial AV-following designs are not string stable. Incorporating string stability into the AV-following design will lead to an over-long following gap headway and thus degrades the driving experience as well as the traffic capacity. A balance point between the string stable headway settings and minimum headway settings, which is closer to the minimum headway settings according to the results, is chosen by vehicle makers to compromise the effects of string instability and traffic capacity.

#### 4.4. Discussions beyond theoretical predictions

Based on the estimated parameters shown in Table 3, Fig. 6 shows how  $\tau$  (i.e., time lag) varies with k (i.e., control sensitivity factor). As shown in Fig. 6, as  $\tau$  increases, k appears decreasing trends for both high speed and low-speed tests. Although the fitted lines for high-speed and low-speed tests almost overlap with each other, the estimation results of k are not consistent over different speed conditions. This finding may indicate that the studied ACC system automatically adjusts the vehicle control sensitivity to fit different driving environments, which have not been reported in the literature. There are two possible reasons for this finding – one is that a shorter time-lag gap (i.e.,  $\tau$ ) requires a stronger control sensitivity (i.e., k) to avoid the following vehicle getting too close to the preceding vehicle, and the other is that since a simple linear AV-following model was adopted by this study, the following behaviors may exceed the predictivity of the model, which opens up future research needs for investigating nonlinearity and stochasticity in AV following modeling.

It was also found in Table 3 that the estimated results for key parameters of the AV following design are not always consistent over different speed ranges; i.e., for the same headway setting, the values of the estimated  $\Delta$  for the high-speed range are greater than those for the low-speed range. This inconsistency may be because that the linear model likely overestimates actual speed oscillation response particularly when the oscillation magnitude gets high (Li and Ouyang, 2011). It indicates that the following behaviors of the studied AV design exceed the predictivity of the adopted simple linear model and thus suggests the needs of a nonlinear AV following model.

# 4.5. Finding verifications

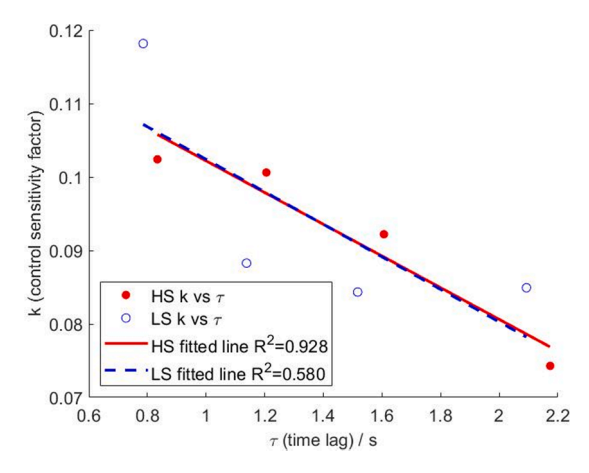
The AV-following data shared by Gunter et al. (2019) offered an opportunity to verify the generality of the major findings in the commercial AV following control design. Gunter et al. (2019) conducted the AV- following trajectory data collection by seven commercial AVs from two types of vehicle makers (e.g., makers 1 and 2), and two headway settings (e.g., long and short) for each AV were tested in the experiment. With this, the following data of one AV from each type of vehicle maker was selected, and a total of two sets of AV-following data were used to fit the AV-following model (I). Similarly, the simple moving average method with a window of 5 s was adopted to denoise the trajectory data before parameter estimations. Estimation results are shown in Table 8.

Table 8 shows that for each vehicle maker, the values of  $\Delta$  increase as  $\tau$  decrease, which verifies the tradeoff between the time lag gap and the safety buffer. Also, the values of  $k\tau^2$  of all estimations are less than 2, indicating that the studied AV following designs still are string unstable. However, as the headway settings (i.e.,  $\tau$ ) increase, the values of  $k\tau^2$  increase as well and thus the AV string stability increases, verifying the relationship between the time lag gap and AV string stability. Moreover, the estimated vehicle control sensitivity factors (i.e., k) also vary across different headway settings, which implicate the need for investigating nonlinearity and stochasticity in AV following modeling. Further, the estimated factors for the three AV-following designs (Lincoln, maker 1, and maker 2) are different, suggesting that the AV-following designs produced by different vehicle makers are inconsistent and thus the traffic flow of pure AVs should still be studied heterogeneously (Shi and Li, 2020).

#### 5. Conclusions

To verify theoretical findings in Li (2020) and study the vehicle following behaviors of commercial AV control design, this study collected field experiment data for AVs. Parameters of the parsimonious linear AV-following model proposed in Li (2020) were estimated with linear regression using the collected trajectory data. Based on the relationship analysis among the estimated parameters (i.e., k,  $\Delta$ ,  $\tau$ ) and the stability analysis, the following theoretical findings were verified:

- 1) There exists a tradeoff between the time lag gap and the safety buffer.
- 2) There exists a relation between the time lag gap and AV string stability.



**Fig. 6.** Scatter plot of  $\tau$  vs k.

Table 8
Estimation Results of Data.

	Maker 1					Maker 2				
	τ(s)	k	Δ(m)	$R_{adj}^2$	$k\tau^2$	τ(s)	k	Δ(m)	$R_{adj}^2$	$k\tau^2$
Headway Setting Long	2.57	0.03	2.99	0.62	0.23	2.11	0.08	3.42	0.60	0.36
Headway Setting Short	1.13	0.04	7.41	0.59	0.05	1.05	0.06	8.59	0.68	0.07

- 3) A possible explanation to the observed string instability of the AV following design is that a relatively short headway (and thus better user experience on vehicle mobility) is set by automakers at a cost of compromising string stability.
- 4) The tradeoff between the mobility and stability can be observed that as the time lag increases, the oscillation period gets longer, and the oscillation amplification gets smaller.

Moreover, the estimated parameters with the field experiment data reveal the following findings beyond that reported in Li (2020):

- 1) The estimated vehicle control sensitivity factors vary across different speed and headway settings.
- 2) The estimated results for key parameters of the AV following design are not consistent over different speed conditions.

One possible reason to this inconsistency is that the following behaviors of the design cannot be fully interpreted by the proposed simple linear model due to the intrinsic limitations of the linear model. Thus, there is a need to investigate nonlinearity and stochasticity in AV following modeling. This inconsistency also reveals that the commercial AV-following design puts much of the safety into the nonlinear control side while the linear control only dominates in a very small speed variation range.

Overall, these findings provide managerial insights into future AV traffic management, and it will be helpful for transportation stakeholders to realize the tradeoffs to better understand the limits and challenges faced in using AV technology to improve traffic performance. Nonetheless, it should be pointed out that this study has several limitations and can be further improved in the following directions. First, this study uses a linear AV following model, though parsimonious, does not consider the speed difference term used in many vehicle following models. Incorporating this term will represent general linearized second-order vehicle controls and further enhance the generality of the analysis. Second, the inconsistent model estimations under different speed conditions reveal the need for investigating nonlinearity and stochasticity in AV following modeling. This also raises cautions of using linear models to describe ACC behavior in simulation, which most traffic simulation does. Moreover, this study looked at the AV-following designs produced by several vehicle makers. More AV longitudinal control designs could be used to validate the proposed findings in future research. Also, it will be interesting to study vehicle-following behavior with incorporating the communication ability of the vehicle and thus the vehicle becomes a connected and automated vehicle, the upgraded version of AV.

# CRediT authorship contribution statement

**Xiaowei Shi:** Methodology, Validation, Formal analysis, Investigation, Data curation, Visualization, Writing - original draft. **Xiaopeng Li:** Conceptualization, Methodology, Validation, Writing - review & editing, Supervision, Funding acquisition.

#### Acknowledgments

This research is sponsored by Susan A. Bracken Faculty Fellowship and National Science Foundation Grants CMMI #1558887 and #1932452. Thanks for the efforts made by other members of the CATS lab in collecting the field experiment data, including Zhaohui Liang, Peng Zhang, Qianwen Li, and Handong Yao. The dataset can be accessed through https://github.com/CATS-Lab-USF.

#### Appendix A

A 5-second moving average filter was adopted to denoise the data. To prove the generality of the findings in this manuscript, we validated our findings with different time spans. The results are attached. It can be seen that the findings are consistent over different filters. Thus, we can conclude that the adopted filter did not impact the main findings presented.

	moving (3 s)			moving (7 s)		
	k	τ	Δ	k	τ	Δ
High Speed-Headway Setting 1	0.10	0.84	4.72	0.09	0.86	4.33
High Speed-Headway Setting 2	0.10	1.20	4.24	0.09	1.24	3.58
High Speed-Headway Setting 3	0.09	1.58	3.14	0.08	1.65	2.41
High Speed-Headway Setting 4	0.07	2.19	0.38	0.07	2.24	0.86
Low Speed-Headway Setting 1	0.12	0.79	7.22	0.10	0.81	7.00
Low Speed-Headway Setting 2	0.09	1.14	6.26	0.08	1.17	5.86
Low Speed-Headway Setting 3	0.08	1.52	5.81	0.07	1.56	5.33
Low Speed-Headway Setting 4	0.08	2.10	4.77	0.07	2.16	3.95

Moving indicates moving average filter, values in brackets are spans.

#### References

Bando, M., Hasebe, K., Nakayama, A., Shibata, A., Sugiyama, Y., 1995. Dynamical model of traffic congestion and numerical simulation. Phys. Rev. E 51, 1035–1042. https://doi.org/10.1103/PhysRevE.51.1035.

Chen, D., Ahn, S., Laval, J., Zheng, Z., 2014. On the periodicity of traffic oscillations and capacity drop: The role of driver characteristics. Transp. Res. Part B Methodol. 59, 117–136. https://doi.org/10.1016/j.trb.2013.11.005.

Eskandarian, A., 2003. Research Advances in Intelligent Collision Avoidance and Adaptive Cruise Control. IEEE Intell. Transp. Syst. Mag. 4, 143–153. https://doi.org/10.1109/TITS.2003.821292.

Ghiasi, A., Hussain, O., Qian (Sean), Z., Li, X., 2017. A mixed traffic capacity analysis and lane management model for connected automated vehicles: A Markov chain method. Transp. Res. Part B Methodol. 106, 266–292. https://doi.org/10.1016/j.trb.2017.09.022.

Gunter, G., Gloudemans, D., Stern, R.E., McQuade, S., Bhadani, R., Bunting, M., Monache, M.L.D., Lysecky, R., Seibold, B., Sprinkle, J., Piccoli, B., Work, D.B., 2020. Are Commercially Implemented Adaptive Cruise Control Systems String Stable? IEEE Trans. Intell. Transp. Syst. 1–12 https://doi.org/10.1109/ TITS.2020.3000682.

Gunter, G., Janssen, C., Barbour, W., Stern, R.E., Work, D.B., 2019. Model based string stability of adaptive cruise control systems using field data. arXiv 5, 90–99. James, R.M., Melson, C., Hu, J., Bared, J., 2019. Characterizing the impact of production adaptive cruise control on traffic flow: an investigation. Transp. B 7, 992–1012. https://doi.org/10.1080/21680566.2018.1540951.

Jerath, K., Brennan, S.N., 2012. Analytical prediction of self-organized traffic jams as a function of increasing ACC penetration. IEEE Trans. Intell. Transp. Syst. 13, 1782–1791. https://doi.org/10.1109/TITS.2012.2217742.

Karaaslan, U., Varalya, P., Walrand, J., 1990. UC Berkeley Research Reports Title Two Proposals To Improve Freeway Traffic Flow Publication Date.

Kesting, A., Treiber, M., Helbing, D., 2010. Enhanced intelligent driver model to access the impact of driving strategies on traffic capacity. Philos. Trans. R. Soc. A Math. Phys. Eng. Sci. 368, 4585–4605. https://doi.org/10.1098/rsta.2010.0084.

Kesting, A., Treiber, M., Schönhof, M., Helbing, D., 2008. Adaptive cruise control design for active congestion avoidance. Transp. Res. Part C Emerg. Technol. 16, 668–683. https://doi.org/10.1016/j.trc.2007.12.004.

Knoop, V.L., Wang, M., Wilmink, I., Hoedemaeker, D.M., Maaskant, M., Van der Meer, E.-J., 2019. Platoon of SAE Level-2 Automated Vehicles on Public Roads: Setup, Traffic Interactions, and Stability. Transp. Res. Rec. J. Transp. Res. Board 2673, 311–322. https://doi.org/10.1177/0361198119845885.

Lenard, M., 1970. Safety Considerations for a High Density Automated Vehicle System. Transp. Sci. 4, 138–158. https://doi.org/10.1287/trsc.4.2.138.

Li, L., Li, X., 2019. Parsimonious trajectory design of connected automated traffic. Transp. Res. Part B Methodol. 119, 1–21. https://doi.org/10.1016/j.trb.2018.11.006.

- Li, X., 2020. Li, X. Trade-off between safety, mobility and stability in automated vehicle following control: An analytical method. 2020. Source: https://www.researchgate.net/publication/343350105\_Trade-off\_between\_safety\_mobility\_and\_stability\_in\_automated\_vehicle\_following\_control\_An\_analytical\_method.
- Li, X., Ouyang, Y., 2011. Characterization of traffic oscillation propagation under nonlinear car-following laws. Transp. Res. Part B Methodol. 45, 1346–1361. https://doi.org/10.1016/j.trb.2011.05.010.
- Li, X., Ouyang, Y., 2010. A continuum approximation approach to reliable facility location design under correlated probabilistic disruptions. Transp. Res. Part B Methodol. 44, 535–548. https://doi.org/10.1016/j.trb.2009.09.004.
- Li, X., Wang, X., Ouyang, Y., 2012. Prediction and field validation of traffic oscillation propagation under nonlinear car-following laws. Transp. Res. Part B Methodol. 46, 409–423. https://doi.org/10.1016/j.trb.2011.11.003.
- Makridis, M., Mattas, K., Ciuffo, B., 2020a. Response Time and Time Headway of an Adaptive Cruise Control. An Empirical Characterization and Potential Impacts on Road Capacity. IEEE Trans. Intell. Transp. Syst. 21, 1677–1686. https://doi.org/10.1109/TITS.2019.2948646.
- Makridis, M., Mattas, K., Ciuffo, B., Re, F., Kriston, A., Minarini, F., Rognelund, G., 2020b. Empirical Study on the Properties of Adaptive Cruise Control Systems and Their Impact on Traffic Flow and String Stability. Transp. Res. Rec. J. Transp. Res. Board 2674, 471–484. https://doi.org/10.1177/0361198120911047.
- Milanés, V., Shladover, S.E., 2014. Modeling cooperative and autonomous adaptive cruise control dynamic responses using experimental data. Transp. Res. Part C Emerg. Technol. 48, 285–300. https://doi.org/10.1016/j.trc.2014.09.001.

Milanes, V., Shladover, S.E., Spring, J., Nowakowski, C., Kawazoe, H., Nakamura, M., 2014. Cooperative adaptive cruise control in real traffic situations. IEEE Trans. Intell. Transp. Syst. 15, 296–305. https://doi.org/10.1109/TITS.2013.2278494.

Naranjo, J.E., González, C., García, R., De Pedro, T., 2008. Lane-change fuzzy control in autonomous vehicles for the overtaking maneuver. IEEE Trans. Intell. Transp. Syst. 9, 438–450. https://doi.org/10.1109/TITS.2008.922880.

Ngoduy, D., 2013. Analytical studies on the instabilities of heterogeneous intelligent traffic flow. Commun. Nonlinear Sci. Numer. Simul. 18, 2699–2706. https://doi.org/10.1016/j.cnsns.2013.02.018.

Qu, X., Yu, Y., Zhou, M., Lin, C.T., Wang, X., 2020. Jointly dampening traffic oscillations and improving energy consumption with electric, connected and automated vehicles: A reinforcement learning based approach. Appl. Energy 257, 114030. https://doi.org/10.1016/j.apenergy.2019.114030.

SAE, 2020. Levels of driving automation are defined in new SAE International standard J3016, 2018. Source: https://goo.gl/gCIFCm.

Seiler, P., Pant, A., Hedrick, K., 2004. Disturbance propagation in vehicle strings. IEEE Trans. Automat. Contr. 49, 1835–1841. https://doi.org/10.1109/TAC.2004.835586.

Shi, X., Li, X., 2020. Constructing Fundamental Diagram for Traffic Flow with Automated Vehicles: Methodology and Demonstration. https://doi.org/10.13140/RG.2.2.25353.67681.

Shi, X., Li, X., 2019. Speed Planning for an Autonomous Vehicle with Conflict Moving Objects. 2019 IEEE Intell. Transp. Syst. Conf. 1-6.

Shladover, S.E., Su, D., Lu, X.Y., 2012. Impacts of cooperative adaptive cruise control on freeway traffic flow. Transp. Res. Rec. 2324, 63–70. https://doi.org/10.3141/2324-08.

Talebpour, A., Mahmassani, H.S., 2016. Influence of connected and autonomous vehicles on traffic flow stability and throughput. Transp. Res. Part C Emerg. Technol. 71, 143–163. https://doi.org/10.1016/j.trc.2016.07.007.

Treiber, M., Kesting, A., 2013. Traffic flow dynamics: Data, models and simulation. Data, Model. Simul, Traffic Flow Dyn.

Wang, Z., Shi, X., Li, X., 2019. Review of Lane-Changing Maneuvers of Connected and Automated Vehicles: Models. J. Indian Inst. Sci, Algorithms and Traffic Impact Analyses.

Xiao, L., Gao, F., 2010. A comprehensive review of the development of adaptive cruise control systems. Veh. Syst. Dyn. 48, 1167–1192. https://doi.org/10.1080/00423110903365910.

Ciuffo, B., Mattas, K., Anesiadou, A., Makridis, M., 2020. Open ACC Database. European Commission, Joint Research Centre (JRC). PID: http://data.europa.eu/89h/9702c950-c80f-4d2f-982f-4dd06ea0009f.